

Author Queries

Journal: Journal of the Royal Society Interface

Manuscript: rsif20230034

As the publishing schedule is strict, please note that this might be the only stage at which you are able to thoroughly review your paper.

Please pay special attention to author names, affiliations and contact details, and figures, tables and their captions.

The corresponding author must provide an ORCID ID if they haven't done so already. If you or your co-authors have an ORCID ID please supply this with your corrections. More information about ORCID can be found at <http://orcid.org/>.

No changes can be made after publication.

SQ1 Please confirm that this paper is intended to be Open Access. The charge for Open Access should be paid before publication. If you have not yet received an email requesting payment please let us know when returning your corrections.

SQ2 Your supplementary material will be published online alongside your article and on rs.figshare.com exactly as the file(s) are provided. Therefore, please could you either confirm that your supplementary material is correct, or – if you have any changes to make to these files – email these along with your proof corrections to the . Your ESM files are listed here for your convenience:

Kim and Hu (2023) Onggi - Supplemental Material.pdf

Supplementary_Figure_1.eps

Supplementary_Figure_2.eps

Supplementary_Figure_3.eps

Supplementary_Movie_1_Time_lapse_Kimchi_fermentation_7days.mp4

Supplementary_Movie_2_Time_lapse_salt_flower_macroscopic_24hours.mp4

Supplementary_Movie_3_Time_lapse_salt_flower_microscopic_2days.mp4

Supplementary_Movie_4_Time_lapse_salt_flower_Leica__microscopic_x3000_scalebar 500um.mp4

Supplementary_Movie_5_CT_scan_visualized_pores.mov

Supplementary_Table_1.png

(2-2) Kim and Hu (2023) Onggi - Supplemental Material.pdf

Q1 Keywords have been taken from the metadata/PDF provided. Please check.

Q2 Please provide author(s) initials and year details for the personal communication.

Q3 Please provide the page range for reference [13].

Q4 Please provide publisher location [city/state/country] for references [15, 18, 27, 29 and 36].

Q5 Please provide book title and publisher details for reference [19].

Q6 Please provide publisher details for reference [21].



Cite this article: Kim S, Hu DL. 2023 Onggi's permeability to carbon dioxide accelerates kimchi fermentation. *J. R. Soc. Interface* 20230034.

<https://doi.org/10.1098/rsif.2023.0034>

Received: 25 January 2023

Accepted: 13 March 2023

Subject Category:

Life Sciences—Physics interface

Subject Areas:

biomathematics, biophysics, biomechanics

Keywords:

permeability, permeance, onggi, kimchi, lactic acid bacteria, fermentation

Author for correspondence:

David L. Hu

e-mail: hu@me.gatech.edu

Electronic supplementary material is available online at rs.figshare.com.

Onggi's permeability to carbon dioxide accelerates kimchi fermentation

SooHwan Kim¹ and David L. Hu^{1,2}

¹Schools of Mechanical Engineering, and ²School of Biology, Georgia Institute of Technology, Atlanta, GA, USA

DLH, 0000-0002-0017-7303

Since ancient times, Korean chefs have fermented foods in an onggi, a traditional earthenware vessel. The porous structure of the onggi mimics the loose soil where lactic acid bacteria is naturally found. This permeability has been purported to facilitate the growth of lactic acid bacteria, but the details of the process remain poorly understood. In this combined experimental and theoretical study, we ferment salted Napa cabbage in onggi and hermetic glassware and measure the time course of carbon dioxide concentration, which is a signature of fermentation. We present a mathematical model for carbon dioxide generation rate during fermentation using the onggi's gas permeability as a free parameter. Our model provides a good fit for the data, and we conclude that porous walls help the onggi to 'exhale' carbon dioxide, lowering internal levels to those favoured by lactic acid bacteria. The positive pressure inside the onggi and the constant outflow through its walls act as a safety valve for bacteria growth by blocking the entry of external contaminants without mechanical components. We hope this study draws attention to the work of traditional artisans and inspires energy-efficient methods for fermenting and storing food products.

1. Introduction

According to ancient texts, Koreans have enjoyed fermented foods since the Goguryeo Kingdom (37 BC–AD 668) [1]. Before the advent of refrigeration, Korean chefs used handmade clay vessels called onggi to ferment their foods. The onggi was designed without modern knowledge of chemistry, microbiology or fluid mechanics. Onggi-shaped vessels are depicted in numerous historical records, such as the tomb mural in [figure 1a](#) from Anak Tomb No. 3, dating back to AD 357 [2]. Many recent studies purport that fermentation in onggi can help preserve and increase the nutrition of fermented foods [3,4]. While modern mass fermentation is performed in controlled conditions such as metal vessels, there remain a number of artisans who continue to make onggi by hand. The goal of this study is to present a mechanical explanation for the ability of onggi to aid in fermentation. We hope that this study will increase the visibility of onggi makers and inspire energy-efficient ways to preserve and ferment foods.

Onggi have traditionally been used to make a variety of fermented food such as kimchi (fermented spicy cabbage, [figure 1b](#)), ganjang (soya sauce), gochujang (red pepper paste) and doenjang (soya bean paste), all of which have become essential parts of Korean cuisine. The addition of salt to these vegetable products, which already contain natural bacteria, prevents spoilage while promoting the proliferation of salt-loving lactic acid bacteria [5,6]. In fact, the signature sour taste of these foods is due to the lactic acid produced by probiotic bacteria including the rod-shaped *Lactobacillus* species (10 μm in length) and oval-shaped *Leuconostoc* species (1 μm in length) [7]. Research on onggi has primarily focused on accelerating the growth of lactic acid bacteria while suppressing the growth of other bacterial strains. Kimchi fermented in onggi over four weeks had 100 times higher lactic acid bacteria counts than kimchi

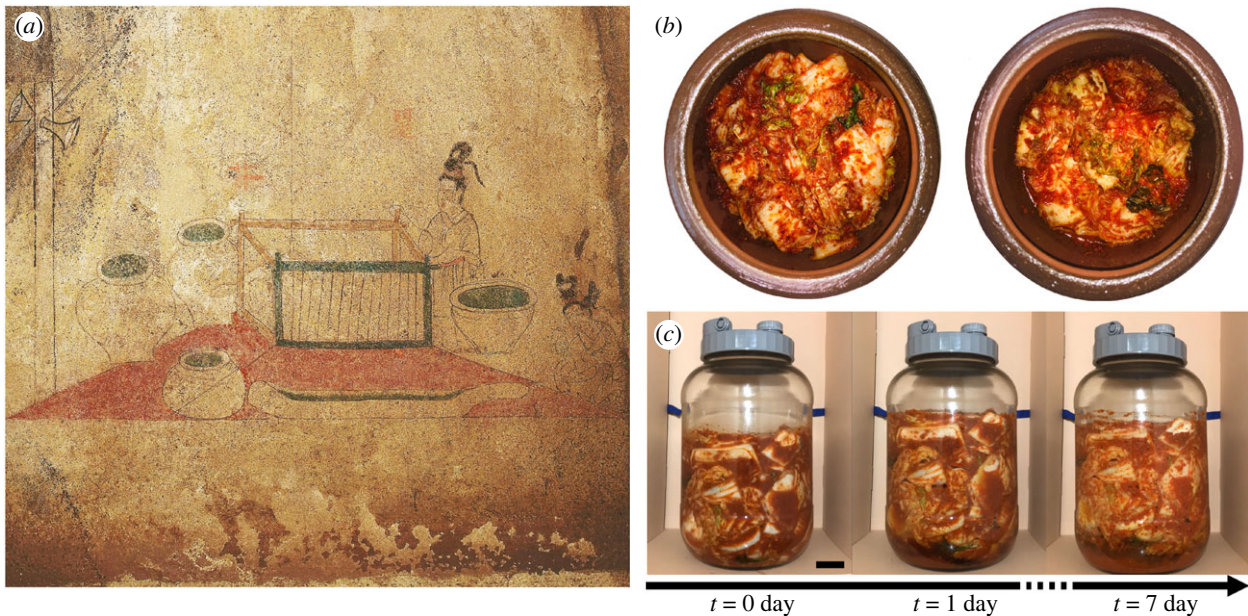


Figure 1. (a) Vessels resembling onggi on a mural at Anak Tomb No. 3 from Goguryeo Kingdom (37 BC–AD 668). Image courtesy of the Northeast Asian History Foundation. (b) Top view of kimchi inside an onggi before (left) and after (right) fermentation. (c) Side view of kimchi fermented in a glass jar for 7 days at 30°C. Scale bar 30 mm. The process of interest is the lactic acid fermentation driven by two species of anaerobic bacteria, *Lactobacillus* and *Leuconostoc*. A dramatic volume increase and the formation of carbon dioxide bubbles were observed within 1 day.

fermented in plastic and steel containers [3]. Moreover, onggi fermentation slowed the growth of foul-tasting aerobic bacteria by a factor of 100. Onggi also increases the acidity and antioxidant activity of kimchi [8,9].

While the improved lactic acid bacteria growth in onggi is exciting, a missing link in this field is a connection between the material properties of the onggi and the growth of bacteria. In this study, we apply the methods of fluid mechanics to determine this connection. We hypothesize that onggi influences fermentation by the transmission of gas through its porous walls. Onggi has numerous gas-permeable micro-pores ranging from 1 to 100 μm in size [10,11]. These pores increase the transmission of oxygen and carbon dioxide with respect to most modern food containers made from polyethylene and glass [3,12]. Many researchers assume that the gas permeability of onggi causes the high bacterial count in fermented food like kimchi, but a clear mechanism has yet to be given. Previous studies only measured the carbon dioxide of an initially gas-filled vessel without living bacteria, or only considered the growth of bacteria without measuring gas generation [3]. In our work, we examined the interaction of fermenting cabbage, the carbon dioxide it generates, and the permeability of its walls. We linked these three subjects using a mathematical model that accounts for the onggi's permeability to carbon dioxide.

Critical to the onggi's function is its permeability, the capacity of a porous material to allow fluids to flow through it. By virtue of its liquid permeability k , onggi generates 'salt flowers', salt crystals that appear on its outside when fermenting salty foods. As we will show, the onggi's gas permeability k_g enables it to transmit the carbon dioxide generated by fermentation. In general, permeability depends on the shape and size of interconnected pores in the material. It is an intrinsic property of porous materials and has traditionally been used to show how water travels through filters, gravel and aquifers. Permeability is defined in units

of area and refers to the area of open space in a cross-section that is perpendicular to the direction of flowing fluid [13,14].

2. Material and methods

2.1. Onggi construction and characterization

In the summer of 2021, we purchased a large onggi from Jeju Onggi Village on Jeju Island, Korea. The onggi had a volume of 4600 ml with a mouth radius of 10 cm and a height of 20 cm. One constraint was that the vessel had to be tall and wide enough to fit our airborne carbon dioxide sensors without touching the cabbage. The onggi was manufactured by a traditional process which we describe here [11]. Raw mud containing water, silt and clay was pressed and slapped by hand to homogenize it. Pebbles were picked out and the material was first formed into long clay rods. Then, the pottery was shaped on a spinning wheel and left for about a day under ambient conditions to dry out. Finally, onggi slowly sintered inside a kiln at around 1200°C for a day and slowly cools down. While some onggi are glazed, ours was not.

We characterized the pore structure with both a scanning electron microscope (Hitachi SU-8010 SEM) and computed tomography (Scanco CT-50). The sample for SEM imaging was prepared using a rotary saw with a diamond wafering blade (PELCO Precision Low-Speed Saw) to obtain a smooth surface. The sample for the CT scan was prepared by breaking it with a hammer. A small piece was mounted on a 6 mm diameter sample holder and imaged under high-resolution settings (55 kV of energy, 145 μA of intensity, 1 s of sample time and 2 μm voxel size). A threshold masking was set to lower and upper limits of 5183 HU (Hounsfield units) and 10 000 HU, respectively. The porosity was computed by sampling multiple cylinders (diameter 600 μm and length 1000 μm) within the boundary of the outer surface.

2.2. Kimchi fermentation time-lapse

For the time-lapse video of fermentation (figure 1c; electronic supplementary material, movie S1), we relied on a traditional

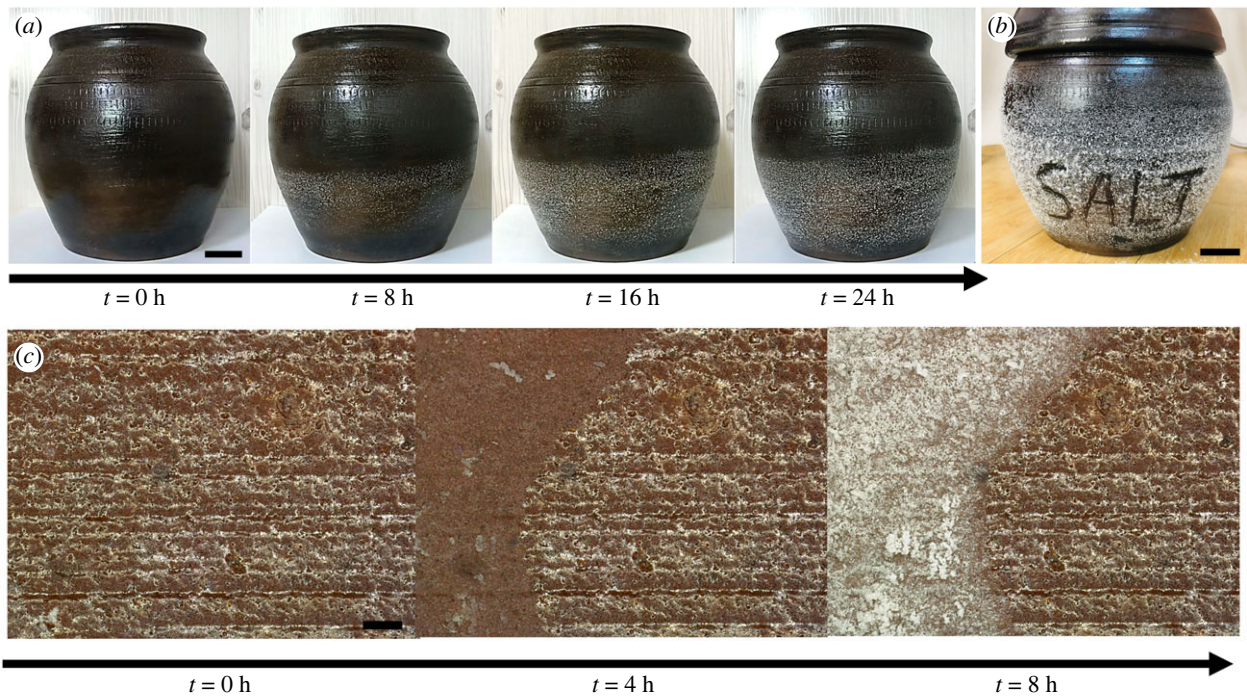


Figure 2. (a) Time-lapse of salt flower formation on the outer surface of an onggi for 24 h. Scale bar 50 mm. (b) Onggi surface covered with salt crystals after 3 days. Scale bar 50 mm. (c) The microscopic time-lapse of salt flower at the outer onggi surface for 8 h. Scale bar 500 μm . Salt crystals form as the evaporation dries out the water contents and fluid is imbibed to the surface.

kimchi recipe. Throughout the study, Napa cabbage (*Brassica rapa* subsp. *pekinensis*) was purchased from local grocery stores, either on Jeju Island or in Atlanta. We used 1 kg of the crispy layers of cabbage for the time-lapse. Each leaf of cabbage was cut into two or three pieces perpendicular to the midrib so that each piece consisted of both the wrinkled lamina and the surrounding veins. The Napa cabbage was immersed in 2 wt% salty water for 6 h and then mixed thoroughly with traditional kimchi seasoning, which for each kg of cabbage consisted of 160 g of powdered red pepper, 200 g of minced onion, 20 g of anchovy fish sauce, 15 g of minced garlic and 5 g of minced ginger.

Kimchi fermentation could not be easily observed in onggi because of the dark conditions inside the vessel. Thus, we conducted the time-lapse video of kimchi fermentation in a hermetically sealed glass jar. The fermentation process was filmed by a USB camera (Logitech Brio 4K Webcam) for seven days at 3°C, illuminated by a single LED source.

2.3. Salt flower formation

Two time-lapse videos of salt crystal formation were performed: one in a macroscopic view and another in a microscopic view. In the macroscopic view (figure 2a,b; electronic supplementary material, movie S2), the onggi was filled with 21 of 15 wt% salty water and observed for 24 h using a USB camera (Logitech Brio 4K Webcam).

For the microscopic film (figure 2c; electronic supplementary material, movies S3,4), a rectangular onggi piece was observed for 2 days while the bottom of the sample was immersed in 15 wt% salty water. This per cent saltwater is comparable to the salt concentration in soy sauce (approx. 18%) which may be fermented in onggi [15]. We used a stereo optical microscope (Leica DVM6 Digital Microscope) in the multi-focus setting.

2.4. Water evaporation measurement

To measure the onggi permeability to water, we measured how quickly water evaporated from its walls. The onggi was initially filled with 2000 g of water and the top was sealed with plastic

stretch wrap and a rubber ring. This set-up ensured that evaporation mostly occurred through the porous walls of the onggi. The time course of the mass was measured by a portable balance (Mettler Toledo PL-E).

2.5. Carbon dioxide measurement

For the carbon dioxide measurements, we applied only saltwater to the cabbage because the kimchi recipe includes ingredients for flavour but salt is the necessary component to stimulate fermentation. We measured the carbon dioxide concentration and estimated the gas production in two containers, a hermetically sealed glass jar and closed-top onggi (figure 4a). For the onggi, we designed and built a custom-fit lid for three types of gas sensors: a pressure sensor, a carbon dioxide sensor, and an oxygen sensor (Vernier Software & Technology). These sensors fit vertically into the onggi mouth using a custom-designed three-dimensional-printed lid (Formlabs Form 3). All purpose sealing film (Bemis, Parafilm) filled any remaining gaps between the devices and the lid. Despite our efforts, our 'hermetically sealed' glass jar leaked, but less so than the permeable onggi, as shown by the factor of two differences in their gas permeability k_g presented in the results section.

We performed three fermentation trials of salted cabbage in a glass jar and an onggi. The glass jar had a volume of 1900 ml, a height of 15 cm and a radius of 10 cm. In each trial, 200 g of cabbage was observed for 2 days. To prepare the salted cabbage for observation, it was first immersed in brine with 2 wt% of salt concentration for 6 h. For all trials, cabbage was drained of water before being placed in the containers for measurement. Unlike traditional kimchi fermentation, there were no extra seasonings in the jars, so the salted cabbage sat without any surrounding liquid, as shown in figure 4a.

The onggi was placed in a laboratory oven (Quincy Lab 30GC Convection Lab Oven), controlled by a voltage regulator (Variac TDGC-0.5KM) to maintain darkness and a temperature of 25°C. While the typical temperature for kimchi fermentation is about 10°C [16], we used a higher temperature to expedite

190 fermentation. Since the containers' pores harbour bacteria [11,17],
191 the containers were sterilized in an autoclave (Steris Amsco
192 Century SV-136H Prevac Steam Sterilizer) before each trial.

193 3. Mathematical models

194 We present mathematical models on the permeability of the
195 onggi to liquids and gases. The former was used to estimate
196 the liquid permeability k and the latter to infer the carbon
197 dioxide generation rate of the lactic acid bacteria. At the
198 end of the section, we enumerate the values of the dimension-
199 less groups used in these models. The dimensionless groups
200 justify the modelling choices made.

201 3.1. Liquid permeability model

202 Our model predicts the liquid permeability k of the onggi wall
203 based on the evaporation rate of water from the onggi. This
204 model follows our experiment in which a capped water-filled
205 onggi loses mass at a steady rate. Based on our observations
206 of salt formation on the outside of the onggi (figure 2), we
207 assume this mass loss is due to water that has imbibed through
208 the porous walls and evaporated from the outside.

209 Based on the flow speeds of water presented in the
210 dimensional analysis section, the flow through the onggi is
211 characterized by incompressibility and a low Reynolds
212 number. We apply Darcy's Law, which is valid for creeping
213 laminar flow at low Reynold's numbers [18,19]. Darcy's
214 Law states that the volumetric flow rate per unit area q is pro-
215 portional to the gradient of pressure, $q \sim \nabla P = \Delta P/d$, where
216 d is the onggi wall thickness. In all,

$$217 q = -\frac{k \Delta P}{\mu d}, \quad (3.1)$$

218 where the constant of proportionality involves the liquid
219 permeability k of onggi, and the water's dynamic viscosity
220 μ . The outside wall of the onggi is at atmospheric pressure.
221 The two driving pressures of the fluid are the water's hydro-
222 static pressure and the capillary pressure which tends to
223 imbibe fluid into the hydrophilic wall. The sum of these
224 two pressures may be written

$$225 |\Delta P| \sim \rho g z + \frac{4\sigma \cos \theta}{d_p}, \quad (3.2)$$

226 where ρ is the density of water, g is gravitational acceleration,
227 z is the height from the water surface, σ is the surface tension
228 of water, θ is the contact angle of water on the onggi and d_p is
229 the pore diameter which we show using microscopy to be on
230 the order of 10 μm . The first term on the right-hand side is the
231 hydrostatic pressure, and the second term is the capillary
232 pressure, or Laplace pressure. The ratio of the hydrostatic
233 term to the capillary term is related to the modified Bond
234 number, which we calculate to be less than 1, indicating the
235 dominance of capillary pressure. We proceed by considering
236 only capillary pressure.

237 We assume a cylindrical container with an effective radius
238 R , which is the average of the onggi mouth radius, maximum
239 radius and bottom radius. The evaporation rate, or the total
240 flow rate integrated across the height of the liquid z_r may
241 be written (figure 3c)

$$242 Q_e \sim 2\pi R \int_0^{z_r} q(z) dz, \quad (3.3)$$

243 where q can be substituted using equations (3.1) and (3.2).
244 Simplifying equation (3.3), we write the liquid permeability
245 k as

$$246 k \sim \frac{\mu d}{2\pi R} \frac{Q_e}{((1/2)\rho g z_r^2 + (4\sigma \cos \theta/d_p)z_r)} \sim \frac{\mu d Q_e d_p}{8\pi R z_r \sigma \cos \theta}. \quad (3.4)$$

247 We may solve equation (3.4) by measuring Q_e from the rate
248 of mass loss of the onggi. The rate of mass loss was converted
249 to a volumetric flow rate using water density. If the evapor-
250 ation rate is measured over a sufficiently small time
251 window, the water height z_r can be considered constant.
252 The model presented applies to liquids passing through
253 the onggi walls. In the next section, we consider the passage
254 of gases.

255 3.2. Gas permeability model

256 The goal of this model is to infer the carbon dioxide generation
257 rate \dot{n}_g (mmol h^{-1}) by the bacteria. This model is necessary
258 because the onggi is permeable to carbon dioxide. Figure 4b
259 depicts the variables used in this model. The primary input
260 to our model is the concentration of carbon dioxide in the
261 vessel C_{CO_2} as measured by our sensor. In order to determine
262 the carbon dioxide generation rate \dot{n}_g (mmol h^{-1}), we con-
263 verted C_{CO_2} to the partial pressure of carbon dioxide in the
264 vessel p_{in} . Note that we used p to denote partial pressure
265 and P to denote the total pressure, which according to Dalton's
266 Law, is the sum of all the partial pressures of the gases (p_{CO_2} ,
267 p_{N_2} , p_{O_2} ...). With this notation, p_{in} and p_{out} are the partial
268 pressures of carbon dioxide inside and outside the vessel.
269 Similarly, P_{in} and P_0 denote the total pressures inside and out-
270 side the vessel. The total pressure in the vessel P_{in} was
271 measured using our pressure sensor. Pressure P_0 and tempera-
272 ture T_0 outside the vessel were given by ambient conditions,
273 which in this case corresponded to a temperature-controlled
274 oven at atmospheric pressure.

275 Conservation of mass states that the rate of change of
276 carbon dioxide in the vessel \dot{n}_{total} (mmol h^{-1}) is the sum of
277 the rates of carbon dioxide outflow \dot{n}_{out} and carbon dioxide
278 generation \dot{n}_g . Note that \dot{n}_{out} is negative, corresponding to
279 carbon dioxide leaving the vessel.

$$280 \dot{n}_{\text{total}} = \dot{n}_{\text{out}} + \dot{n}_g. \quad (3.5)$$

281 The rate of outflow is dictated by the gas permeance
282 equation, which is equivalent to Darcy's Law and states
283 that the molar flow rate is proportional to the pressure gradi-
284 ent. In a porous vessel (figure 5b), the gas permeance
285 equation may be written [3]

$$286 \dot{n}_{\text{out}} = \bar{K} \frac{A}{d} (p_{\text{out}} - p_{\text{in}}), \quad (3.6)$$

287 where \bar{K} is the gas permeance, A is the vessel surface area, d
288 is the vessel wall thickness and p_{out} and p_{in} are the partial
289 pressures of carbon dioxide outside and inside the vessel,
290 respectively. The partial pressure of carbon dioxide
291 outside the vessel is dictated by atmospheric conditions and
292 is given in table S1 in the electronic supplementary material.
293 Carbon dioxide flows out of the vessel if the outflow of
294 carbon dioxide \dot{n}_{out} is negative. This is the case for an
295 onggi fermenting kimchi where the pressure building up
296 inside the vessel exceeds the pressure outside: p_{in} is higher
297 than p_{out} .

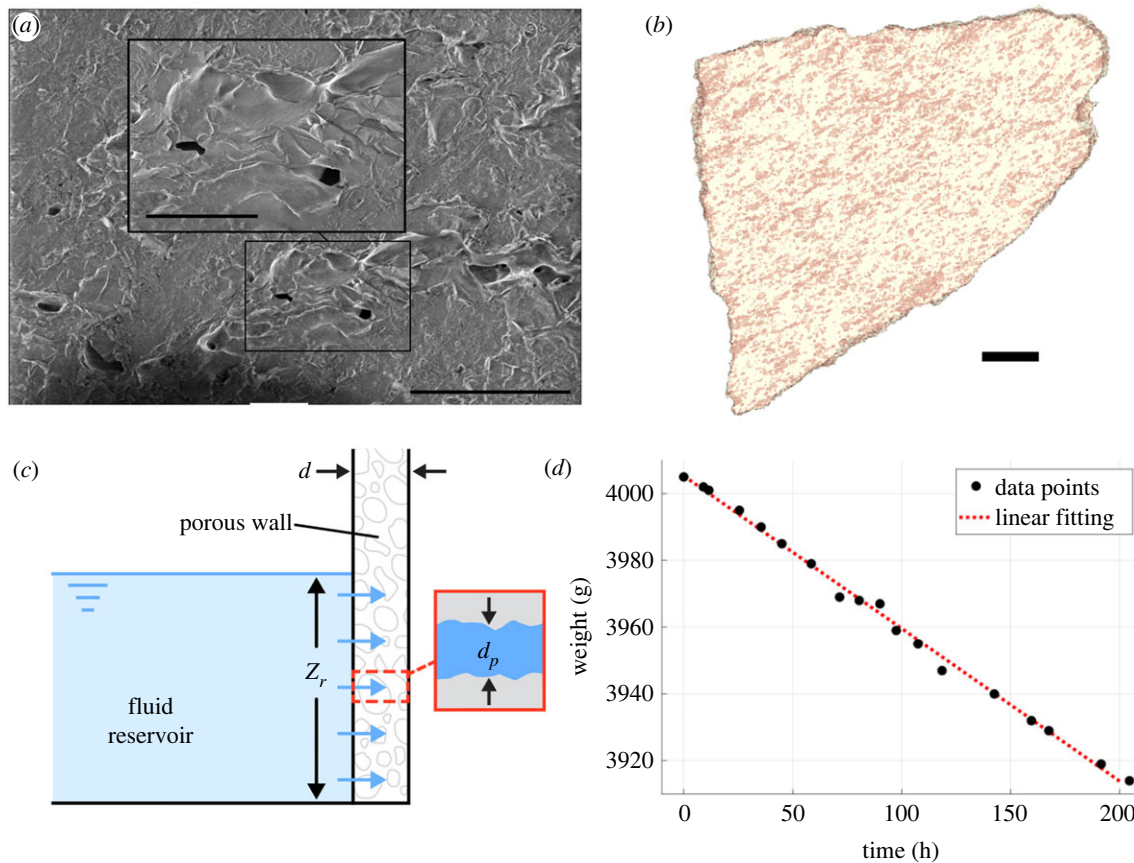


Figure 3. (a) Scanning electron microscope view of micro-pores in onggi. Scale bar, 50 μm. Inset scale bar, 20 μm. Pore size varies from 1 to 100 μm diameter with an average of 5 μm. Additional SEM images can be found in electronic supplementary material, figure S1. (b) Three-dimensional model of a 40 μm-thick onggi slice using computed tomography (CT) scan. Scale bar, 200 μm. Pores are pink and onggi clay is transparent. (c) Schematic of water flow through the porous wall. (d) Time course of the weight of the onggi due to evaporation at the onggi surface.

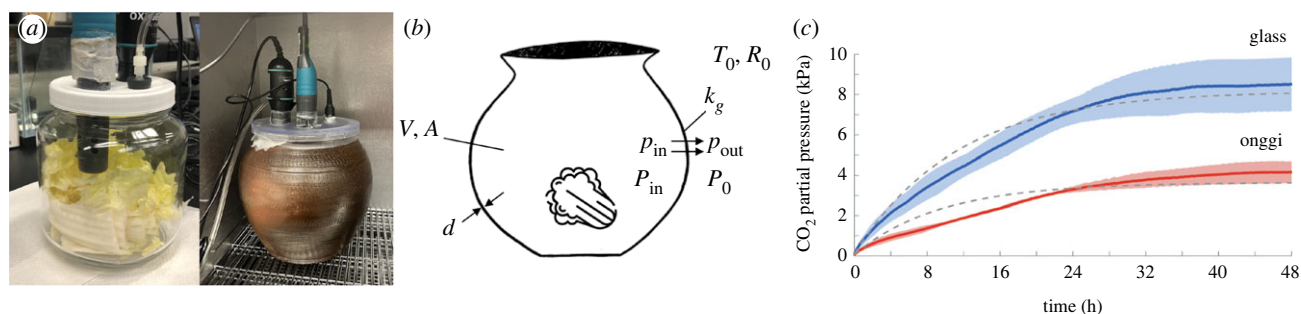


Figure 4. (a) Headspace gas set-up for measuring carbon dioxide, oxygen and pressure in a hermetic glass container (left, 1900 ml of volume) and onggi (right, 4600 ml of volume). (b) Schematic of carbon dioxide generation. Cabbage and jar icons from Flaticon and Clipart Library, respectively. (c) Time course of the carbon dioxide partial pressure for 200 g of salted cabbage stored in glass (in blue) and onggi (in red). Solid lines are from experiments and the dashed lines are from the theoretical model. Raw data are given in electronic supplementary material, figure S2.

The gas permeance of the vessel is defined in terms of the gas permeability and conditions outside the vessel

$$\bar{K} = \frac{P_0}{R_0 T_0} \frac{k_g}{\mu_{\text{CO}_2}}, \quad (3.7)$$

where k_g is the gas permeability of the vessel, P_0 is the ambient pressure, T_0 is ambient temperature, R_0 is the gas constant and μ_{CO_2} is the dynamic viscosity of carbon dioxide at the prescribed pressure and temperature. Note that equation (3.7) is arbitrary in that it neglects the conditions inside the vessel. However, this assumption does not affect our final solution since we will be using k_g as a free parameter.

Before we proceed, we provide a brief cautionary note on the use of gas permeance \bar{K} . In the kimchi fermentation literature, authors may inadvertently interchange the terms permeability, permeance and permeation [3,11,20]. In other fields, confusion between these terms is also common [14]; in fact, some researchers define gas permeance as \bar{K}/d , where d is the wall thickness. In our study, gas permeance is defined in terms of molecules of gas moving unit length that pass a cross-sectional area per hour at a given pressure on the outside of the wall. Thus, permeance has a unit of $\text{mol} \cdot \text{kPa}^{-1} \cdot \text{m}^{-1} \cdot \text{h}^{-1}$, but it is dependent on the intrinsic gas permeability of the material, which has a unit of m^2 [21–23]. We set the gas permeability k_g as a free parameter

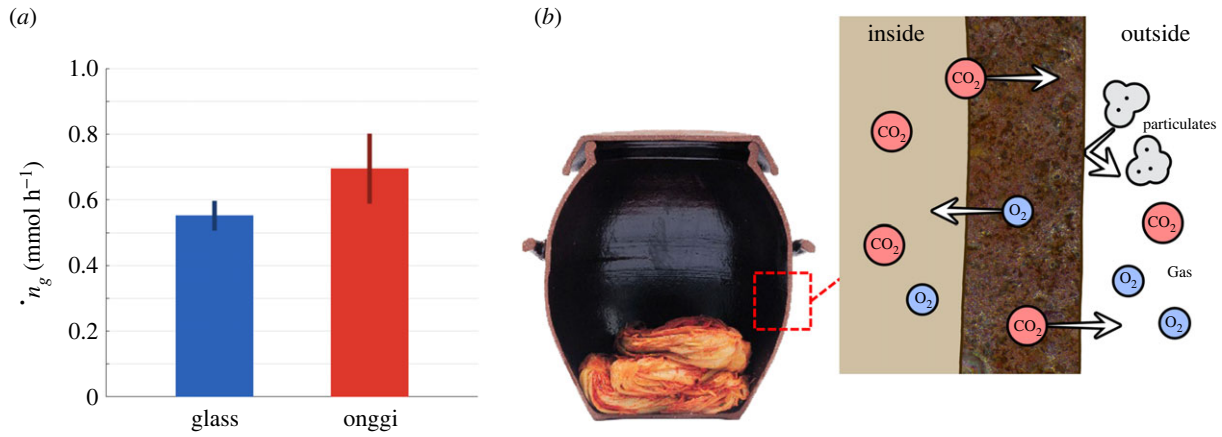


Figure 5. (a) Carbon dioxide generation rates of salted cabbage in glass and onggi, as calculated with our theoretical model. Salted cabbage in onggi generated 25% more carbon dioxide than in glass. (b) Schematic of selective permeability of onggi. The porous onggi wall allows carbon dioxide to exit and oxygen to enter. It also blocks the passage of unwanted particulates larger than the pore size of 5 μm . Onggi cross-section image from Korean Ministry of Culture, Sports and Tourism.

then proceed by presenting the relationships between gas permeability and partial pressures of carbon dioxide.

The partial pressure of carbon dioxide p_{in} inside the vessel is given by the ideal gas law which states that p_{in} is proportional to n_{total} the number of moles of carbon dioxide inside the vessel:

$$p_{\text{in}}V = n_{\text{total}}R_0T_0, \quad (3.8)$$

where V is the vessel volume, T_0 is ambient temperature, and R_0 is the ideal gas constant. Note, here we assume that the temperature inside the vessel is the same as that outside, which is supported by our temperature measurements. The partial pressure of carbon dioxide (in kPa) is simply the product of carbon dioxide concentration C_{CO_2} (in ppm), the total pressure (in kPa), and a constant to convert ppm to a proportion:

$$p_{\text{in}} = C_{\text{CO}_2} \cdot (1 \times 10^{-6}) \cdot P_{\text{in}}. \quad (3.9)$$

Further constants are given in table S1 in the electronic supplementary material.

By assuming p_{out} and \dot{n}_g are constant, we may rewrite equation (3.8) using equations (3.5)–(3.7) in terms of the variable p_{in}

$$\frac{dp_{\text{in}}}{dt} = k_g \frac{P_0 A}{\mu_{\text{CO}_2} V d} (p_{\text{out}} - p_{\text{in}}) + \frac{R_0 T_0}{V} \dot{n}_g \quad (3.10)$$

The initial condition of p_{in} is the partial pressure of carbon dioxide in the ambient. This differential equation may be solved to find the time course of the partial pressure of carbon dioxide inside the vessel

$$p_{\text{in}} = p_{\text{out}} + \beta \left(1 - \exp\left(-\frac{t}{\tau}\right) \right), \quad (3.11)$$

where the time constant τ is

$$\tau = \frac{\mu_{\text{CO}_2} V d}{k_g P_0 A}, \quad (3.12)$$

and the plateau value of p_{in} is influenced by the constant

$$\beta = \frac{\dot{n}_g \mu_{\text{CO}_2} R_0 T_0 d}{k_g P_0 A}. \quad (3.13)$$

Thus, the carbon dioxide generation rate \dot{n}_g influences only the steady-state plateau without influencing the time

constant. Equation (3.11) is the primary tool that we will use to measure the carbon dioxide generation rate from the time course of carbon dioxide data in the onggi headspace.

We collected six total experimental curves for two separate conditions: salted cabbage in each of the onggi and glass containers. Figure 4c shows the average of three trials per condition. The fitting was conducted in MATLAB and OriginPro based on the least-square method. There exist two free parameters: k_g and \dot{n}_g . Optimal k_g values for each of the glass and onggi containers were obtained using a MATLAB code that minimizes the mean of the R^2 values for the datasets. Then, OriginPro produced the associated \dot{n}_g values with uncertainties.

3.3. Dimensionless groups

Our mathematical modelling relied on dimensionless groups, which we calculate using our experimental results below. These dimensionless groups justify our choices in mathematical modelling. A small Reynolds number supports Darcy's law, and a small Bond number reinforces the capillary force dominance, simplifying the calculations for liquid permeability in equation (3.4).

We begin with characteristic velocities and length scales that are relevant for liquid and airflow through the pores of onggi. Using microscopy, we found the pores in the onggi wall had a characteristic diameter of $d_p = 10 \mu\text{m}$. The characteristic velocity U_w for water flow through onggi was obtained by dividing the volumetric flow rate per unit area by the porosity: using equation (3.1), $U_w = q_w / \epsilon \sim 50 \text{ m s}^{-1}$, where we converted porosity converted from percentage to proportion.

To calculate the characteristic velocity of carbon dioxide, we use a combination of equation (3.6), and the time derivative of the ideal gas law applied to the outgoing carbon dioxide \dot{n}_{out} , which is calculated from the experiment

$$P_0 \dot{v} = \dot{n}_{\text{out}} R_0 T_0, \quad (3.14)$$

where \dot{v} is the volumetric flow rate of carbon dioxide. This equation, along with the surface area A of the onggi yields the volumetric carbon dioxide flow rate per unit area $q_{\text{gas}} = \dot{v} / A$. Onggi's characteristic permeability to carbon dioxide, as measured in experiments was $k_g = 6.12 \times 10^{-15} \text{ m}^2$.

379 Consequently, using equation (3.1) again, the characteristic
380 velocity of the carbon dioxide was $U_{\text{gas}} = q_{\text{gas}}/\epsilon \sim 1.9 \text{ m s}^{-1}$.

381 The Reynolds number is defined as

$$382 \quad \text{Re} = \frac{Ud_p}{\nu}, \quad (3.15)$$

383 where U is the velocity of the fluid (either U_w or U_{gas}) and ν is
384 the kinematic viscosity of the fluid. The Reynolds numbers
385 for the water and carbon dioxide flow are 10.4×10^{-4} and
386 5.0×10^{-6} , respectively. Both liquid and gas flow are in the
387 creeping regime, which indicates fluid flow is laminar and
388 inertia-free.

389 The driving force of water flow through the onggi
390 walls is capillarity. Capillary pressure in a pore may be
391 estimated as $P_c = 4\sigma\cos\theta/d_p \sim 24.9 \text{ kPa}$, which is much
392 higher than the measured steady-state gas pressure for
393 fermenting salted cabbage in the onggi, 4.1 kPa . The modi-
394 fied Bond number may be defined as the ratio of the
395 hydrostatic pressure $\rho g z_r$ and the capillary pressure at the
396 pores σ/d_p . Note that there are two length scales at play
397 here, which lead to

$$398 \quad \text{Bo} = \frac{\rho g z_r}{\sigma/d_p}. \quad (3.16)$$

399 The Bo is calculated to be 0.14, which implies that the water
400 imbibition at the onggi pores is dominated by capillarity.

407 4. Results

408 We used several cabbage preparations in this study. The first
409 was 'kimchi cabbage' which involves Napa cabbage (*Brassica*
410 *rapa* subsp. *pekinensis*) and traditional kimchi seasonings. The
411 fermentation of kimchi cabbage was captured by time-lapse
412 video. The second preparation was 'salted cabbage' which
413 only involves cabbage, salt and no other seasonings. The
414 salted cabbage was used in fermentation experiments in
415 which carbon dioxide is measured. The salted preparation
416 was performed over six times. For convenience, we provided
417 the minimal ingredients to trigger fermentation.

418 We filmed kimchi fermentation for 7 days (figure 1c; elec-
419 tronic supplementary material, movie S1). After 24 h of
420 fermentation, the solution increased by 500 ml, which was
421 approximately 10% of the initial liquid, and comparable to
422 half of the volume of the original cabbage (which weighed
423 1 kg). Throughout the next few days, the cabbage generated
424 bubbles, presumably carbon dioxide due to the metabolism
425 of lactic acid bacteria which appears naturally on the cabbage.
426 The changing carbon dioxide in the vessel may in turn influ-
427 ence the growth of the bacteria. We proceed by characterizing
428 the porosity and liquid permeability of the onggi wall, before
429 turning to its gas permeability.

430 Onggi releases gas through its permeable wall, which we
431 characterized using SEM microscope and CT scan. Figure 3a
432 shows the SEM image of a cross-section of the onggi wall.
433 Pore diameters ranged from 1 to 100 μm , which is compar-
434 able to the range of 20 – 150 μm (accounting for 93.04% of
435 the pores) reported by Kim *et al.* [24]. Onggi pore formation
436 is driven by variables in the manufacturing process such as
437 the composition of ingredients, sintering temperature, and
438 sintering time. In comparison, porcelain's ingredients and
439 processing cause its uniformly fine particles to be imperme-
440 able to gas [24].

We used a CT scanner to measure the porosity of the
sample. Since the CT scan resolution was 2 μm voxel size, it
could not resolve pores smaller than this size. Threshold
masking produced a solid three-dimensional model of an
onggi piece (figure 3b; electronic supplementary material,
movie S5). We found a porosity of $\epsilon = 4.72 \pm 0.16\%$, which
is comparable to $7.21 \pm 0.30\%$, measured using mercury poro-
sometry [11], and four times smaller than $18.71 \pm 0.08\%$, the
average value reported in Seo *et al.* [20]. We note that these
other workers used indirect measurements of porosity
through chemical absorption, while ours is a visualization
of the porous structure using X-rays.

We next performed water evaporation experiments
to measure onggi's permeability to liquids. When Korean
chefs ferment ganjang (soya sauce) in onggi, salt crystals pre-
cipitate on the outside of the container, a phenomenon
known as 'salt flower'. We demonstrated this process by film-
ing an onggi halfway full of salty water (figure 2a,b; elec-
tronic supplementary material, movie S2). Within 8 h, a white layer
of salt crystals appears on the outside, intensifying over time.
Salt is initially limited to the water line but climbs above it
after 24 h. Chefs (Onggi Village pers. comm.) believe the
appearance of the salt flower indicates a good quality fer-
mentation vessel.

To better visualize the salt flower formation, we per-
formed time-lapse videography of a small piece of onggi
atop salt water using a microscope. Figure 2c and electronic
supplementary material, movies S3,4 show a dry outer wall
covered by a thin film of water and then by salt crystals.
Based on these events, we surmise that salt water flows
through the wall and evaporates at the outer surface, leaving
salt crystals behind. Evaporation of water at the outer surface
is replenished by water wicked through the wall.

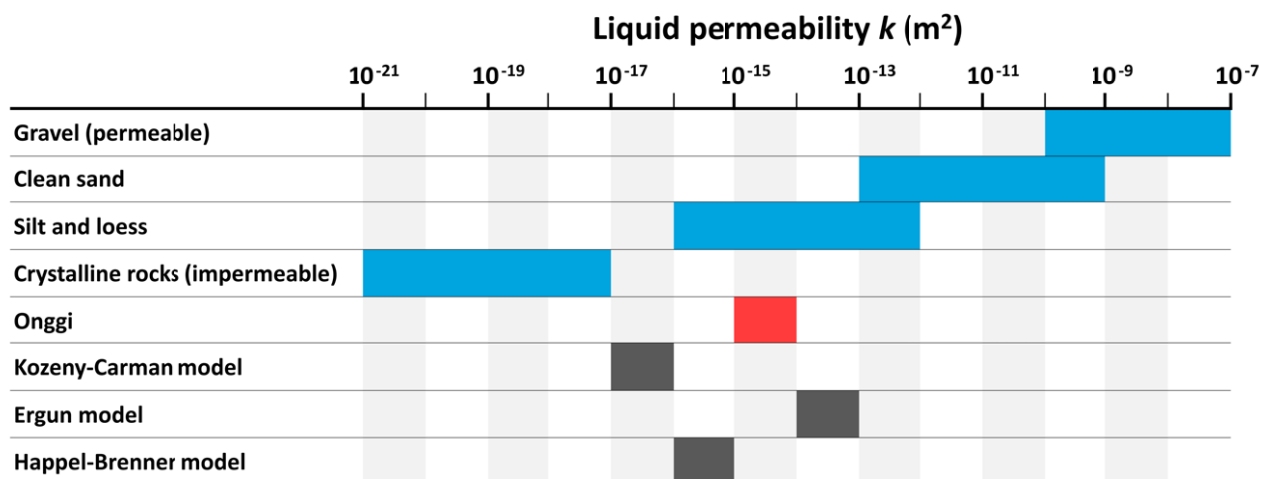
Now that we see onggi is permeable to water, we measure
the flow rate. We filled the onggi with 2000 g of water and
sealed the top. The water flowed through the walls and evap-
orated at a constant rate of $Q_e = 0.75 \pm 0.18 \text{ g h}^{-1}$ ($R^2 = 0.989$)
as shown in figure 3d. Using equation (3.4), we estimate the
liquid permeability of the onggi sample to be $k = (4.58 \pm$
 $1.10) \times 10^{-15} \text{ m}^2$. Converting liquid permeability to hydraulic
conductivity $K = k\rho g/\mu$ yields $K = (4.58 \pm 1.10) \times 10^{-8} \text{ m s}^{-1}$,
where ρ is the density of water, g is the acceleration of gravity
and μ is the dynamic viscosity of water [25]. Table 1 compares
the liquid permeability of onggi with other well-characterized
geological materials that are not tested here, but simply
included for comparison. Onggi is comparable to silt and
loess (a layer of windblown dust and silt covering 10 per
cent of the earth). This makes sense since onggi is made
mainly from natural mud, which has silt as a large com-
ponent. We classify onggi as semi-permeable because it lies
between permeable materials such as clean sand and gravel
($k \sim 10^{-7} - 10^{-10} \text{ m}^2$) and impermeable materials such as
granite ($k \sim 10^{-17} - 10^{-21} \text{ m}^2$).

We may also compare the measured liquid permeability
to predictions from theoretical models [27–29]

$$441 \quad \left. \begin{aligned} \text{Kozeny – Carman model: } k &= \frac{d_{\text{par}}^2}{180} \cdot \frac{\epsilon^3}{(1-\epsilon)^2}, \\ \text{Ergun model: } k &= \frac{1}{66.7} \cdot \epsilon d_{\text{par}}^2 \\ \text{and Happel – Brenner model: } k &= \frac{2}{9} d_{\text{ch}}^2 \cdot \frac{2-(9/5)(1-\epsilon)^{1/3}-\epsilon-(1/5)(1-\epsilon)^2}{1-\epsilon} \end{aligned} \right\} \quad (4.1)$$

where ϵ is the porosity, d_{par} is the particle diameter, d_{ch} is the
channel diameter and other coefficients are empirically

Table 1. Onggi permeability compared to other geological materials and predictions from mathematical models. Onggi permeability is in the middle of the conventional range of permeable and impermeable materials. Data on rocks and sediments from [25,26].



found. Table 1 also shows the calculated permeability based on these models, assuming d_{par} and d_{ch} equal to the pore size of 10 μm , and ϵ equals 4.72 %. These models all give values within 3 orders of magnitude of our measurement, which was on the order of 10^{-15} . Ergun and Happel–Brenner models appear the most accurate, differing by only a factor of 100 from our measurement. We conclude that the onggi wall is indeed a semi-permeable barrier to liquids. We proceed by studying the effect of this permeability to carbon dioxide on fermentation.

We investigate the carbon dioxide generated by salted Napa cabbage placed in an onggi and a glass jar. We perform three experiments for each container and report the average time course of carbon dioxide. We assumed that the salted cabbage had negligible cellular respiration and generated carbon dioxide mainly through bacterial fermentation. Using equation (3.9), we converted carbon dioxide concentration to partial pressure. Figure 4c shows the time course of the partial pressure of carbon dioxide for salted cabbage, where the red line denotes onggi experiments and the blue line denotes glass jar experiments. The onggi's permeable wall clearly permits carbon dioxide to escape, resulting in a slower increase in carbon dioxide and a lower plateau level. Through the lens of our mathematical modelling, we will see that the onggi involves greater carbon dioxide generation than the glass container.

The main challenge with interpreting these results is that the carbon dioxide generation rate is not explicitly known since carbon dioxide is escaping the onggi's permeable walls. To proceed further, we apply our mathematical model, equation (3.11), to calculate the carbon dioxide generation rate \dot{n}_g corresponding to each experiment. We constrain our model with two conditions (1) to have a constant gas permeability for each container and (2) to minimize the error with respect to the time course of experimental carbon dioxide. The modelling shows a good fit to our experimental results, with R^2 values of 0.954 and 0.850, respectively, for glass and onggi. In the electronic supplementary material, we also show tests of cellular respiration for unsalted cabbage.

Our calculation showed the glass container had a gas permeability k_g of $0.796 \times 10^{-18} \text{ m}^2$, while the onggi had more than double the value at $1.701 \times 10^{-18} \text{ m}^2$. We surmise that the permeability of the glass container was due to leaks from the three-dimensional-printed top. Since the onggi had a similarly manufactured top, its increased permeability was likely due to its porous walls. Previous researchers showed that the gas permeability of onggi depends on the glazing treatment, raw ingredients, and the kind of gas [3,20]. They presented permeance values only so we convert our permeability to permeance using equation (3.7). Previously measured gas permeance values for unglazed onggi lie between 0.68 and $19.75 \times 10^{-5} \text{ mol kPa}^{-1} \text{ m}^{-1} \text{ h}^{-1}$, which are on the same order of magnitude compared with our results, $1.70 \times 10^{-5} \text{ mol kPa}^{-1} \text{ m}^{-1} \text{ h}^{-1}$.

Figure 5a shows the calculated carbon dioxide generation rates (mmol h^{-1}) for onggi and glass containers. Salted cabbage carbon dioxide generation rates were $0.552 \text{ mmol h}^{-1}$, for glass and $0.695 \text{ mmol h}^{-1}$ for onggi. Thus, salted cabbage in onggi generated 26% more carbon dioxide than in the glass container, indicative of 26% more bacterial proliferation in the onggi. One-tailed t -test shows this difference was significant ($P = 0.0498$). Moreover, our carbon dioxide generation rates are also comparable to previous measurements. Given the carbon dioxide molecular mass of 44.01 g mol^{-1} , carbon dioxide generation rates per unit mass of cabbage for the glass and onggi were $2915 \text{ mg kg}^{-1} \text{ day}$ and $3670 \text{ mg kg}^{-1} \text{ day}$, respectively, which were similar to that of fermenting kimchi in glass containers, $2531 \text{ mg kg}^{-1} \text{ day}$ under 25°C and 2 wt% salt contents [30].

In conclusion, permeable onggi permits carbon dioxide to escape the container, which in turn accelerates the rate of fermentation. Porosity thus acts as a safety valve for carbon dioxide, maintaining its levels at less than half the values of hermetically sealed containers. Unlike a mechanical valve, there are no moving parts to break. The many pores permit a continuous outflow of gas, which helps reduce the entry of external contaminants. This one-way flow is shown schematically in figure 5b. In comparison to the passive gas control of the onggi, modern fermentation

vessels use manual valves or other mechanical means to allow gas to escape.

5. Discussion

We discuss a few assumptions and caveats to be taken with our salted cabbage experiments. We assumed that the addition of salt to the cabbage triggered fermentation while impeding cellular respiration. Plants exposed to saline conditions experience physiological stress, disruptions to major biochemical processes, and inhibited mitochondrial activity [31,32]. While salt-tolerant plant species can maintain cellular respiration in saline conditions, we assume in this study Napa cabbage has inhibited cellular respiration under high salinity.

Given the high division rate of bacteria compared to plant cells, we infer that increases in carbon dioxide generation are due to bacterial proliferation. Since we cannot distinguish lactic acid bacteria from other bacteria, we assume that the increase in carbon dioxide is due to increased lactic acid bacteria alone. Our assumption is helped by the fact that salt supports lactic acid bacteria growth over other strains.

In our evaporation experiments, we found that onggi's permeability can maintain most of the liquid inside while releasing the gases generated from fermentation. This ability to be semi-porous is a unique feature compared to other potteries. In comparison, terra cotta, a common pottery for houseplants, quickly leaks any water poured into it. For plants, this property may be favourable by preventing the roots from sitting in stagnant water, but it's clearly poorly suited for fermentation, a process where fermented vegetables should be kept moist.

The onggi in this study was unglazed. The traditional way to make onggi glaze is using natural ingredients such as water, tree ash and humus (leaf mould and soil), which come from rotten grass and fallen leaves [3]. While the glaze is aesthetically pleasing, we surmise that it would reduce permeability and in turn reduce its fermentation ability.

Our goal with designing the cover of the glass container was to make it hermetically sealed, but from our modelling, we find the glass container still had half the gas permeability of the onggi. We did not further improve the design because our focus in this study was on the onggi. For simplicity, we modelled both glass and onggi containers as having constant permeability. However, the permeability might be a function of pressure difference. For example, the glass container may be hermetic below a critical pressure, but then permeable as pressure increases. In fact, such nonlinear behaviour is how mechanical relief valves work: they have an energy storage mechanism in the form of a spring or gravity so that gas escapes when a critical pressure is reached.

The glass container only had half the volume of the onggi, and this difference may have influenced the bacteria's activity. Our mathematical model uses the container volume as a parameter to calculate the carbon dioxide partial

pressure. However, the volume of the glass container could affect the interaction between the lactic acid bacteria and carbon dioxide. For example, if the container is large, the carbon dioxide may be diluted to a point where bacteria cannot detect any change. Such behaviour may provide an alternative explanation for the results observed.

Another assumption was a constant carbon dioxide generation rate \dot{n}_g , which reflects the average carbon dioxide rate generated by the lactic acid bacteria in the experimental interval of 48 h. In reality, the bacteria population will increase with time, and so will the carbon dioxide generation rate. However, we did not explore this scenario because it would require knowledge of the doubling time of the bacteria as well as their carbon dioxide generation.

The onggi is just one of many types of fermentation vessels [33,34] and cooking techniques [35,36] with ancient origins. Traditional fermentation vessels like oak barrels or amphora are mainly used for yeast-fermentation of alcoholic beverages, and especially the wooden barrels add flavour by ageing [37,38]. Onggi were designed to promote lactic acid fermentation, which provides the unique taste of kimchi.

6. Conclusion

We used fluid mechanics techniques to show that the onggi continuously 'breathes' carbon dioxide during fermentation, an idea that has been hypothesized for centuries, but had not been directly measured. We find that the onggi's porous walls are permeable to carbon dioxide, which reduces the carbon dioxide level inside the vessel. We surmise that this low carbon dioxide level is favoured by lactic acid bacteria, leading to their greater proliferation, and the increased carbon dioxide generation observed relative to hermetic glass containers. Our mathematical model predicts gas permeability that matches the range of previously reported values for onggi. We hope that this work draws interest to ancient cooking and food preparation strategies.

Data accessibility. The data and code supporting the findings of this study are available from the Github repository: <https://github.com/Delicate-Kim/2023>.

The data are also provided in electronic supplementary material [39].

Authors' contributions. S.K.: conceptualization, data curation, formal analysis, investigation, methodology, project administration, software, validation, visualization, writing—original draft; D.L.H.: funding acquisition, resources, supervision, writing—review and editing.

All authors gave final approval for publication and agreed to be held accountable for the work performed therein.

Conflict of interest declaration. We declare we have no competing interests.

Funding. This material was supported by the Woodruff Faculty fellowship and the NSF Physics of Living Systems student network.

Acknowledgements. We appreciate Christopher Zhang (Brian Hammer Lab) and Pablo Bravo (Peter Yunker Lab) for their initial work on growing lactic acid bacteria. We also thank Laxminarayanan Krishnan in Georgia Tech for CT scan support. Finally, we thank Deok-Saeng Kang for teaching how to make kimchi.

References

- Lee CH, Ahn BS. 1995 Literature review on Kimchi, Korean fermented vegetable foods-I. History of Kimchi making. *J. Korean Soc. Food Cult.* **10**, 311–319.
- Lena K. 2010 Koguryo Tomb murals: world cultural heritage. ICOMOS - Korea Cultural Heritage.

- 568 3. Jeong JK, Kim YW, Choi HS, Lee DS, Kang SA, Park KY. 2011 Increased quality and functionality of kimchi
569 when fermented in Korean earthenware (onggi).
570 *Int. J. Food Sci. Technol.* **46**, 2015–2021. (doi:10.
571 1111/j.1365-2621.2011.02710.x)
- 572 4. Florou-Paneri P, Christaki E, Bonos E. 2013 Lactic
573 acid bacteria as source of functional ingredients. In
574 *Lactic acid bacteria-R&D for food, health and*
575 *livestock purposes*. IntechOpen.
- 576 5. Chao SH, Wu RJ, Watanabe K, Tsai YC. 2009
577 Diversity of lactic acid bacteria in suan-tsai and fu-
578 tsai, traditional fermented mustard products of
579 Taiwan. *Int. J. Food Microbiol.* **135**, 203–210.
580 (doi:10.1016/j.jfoodmicro.2009.07.032)
- 581 6. Yang X, Hu W, Xiu Z, Jiang A, Yang X, Saren G, Ji Y,
582 Guan Y, Feng K. 2020 Effect of salt concentration on
583 microbial communities, physicochemical properties
584 and metabolite profile during spontaneous
585 fermentation of Chinese northeast sauerkraut. *J. Appl.*
586 *Microbiol.* **129**, 1458–1471. (doi:10.1111/jam.14786)
- 587 7. Dharaneedharan S, Heo MS. 2016 Korean
588 traditional fermented foods—a potential resource of
589 beneficial microorganisms and their applications. *J. Life*
590 *Sci.* **26**, 496–502. (doi:10.5352/JLS.2016.26.4.496)
- 591 8. Park S, Lee S, Park S, Kim I, Jeong Y, Yu S, Shin SC,
592 Kim M. 2015 Antioxidant activity of Korean
593 traditional soy sauce fermented in Korean
594 earthenware, Onggi, from different regions.
595 *J. Korean Soc. Food Sci. Nutr.* **44**, 847–853. (doi:10.
596 3746/jkfn.2015.44.6.847)
- 597 9. Lee KS, Lee YB, Lee DS, Chung SK. 2006 Quality
598 evaluation of Korean soy sauce fermented in Korean
599 earthenware (Onggi) with different glazes.
600 *Int. J. Food Sci. Technol.* **41**, 1158–1163. (doi:10.
601 1111/j.1365-2621.2006.01161.x)
- 602 10. Seo GH, Song BS, An DS, Chung SK, Lee DS. 2006
603 Physical properties of Korean earthenware (Onggi)
604 as food container. *Korean J. Packaging Sci. Technol.*
605 **12**, 87–90.
- 606 11. Seo GH, Yun JH, Chung SK, Park WP, Lee DS. 2006
607 Physical properties of Korean earthenware
608 containers affected by soy sauce fermentation use.
609 *Food Sci. Biotechnol.* **15**, 168–172.
- 610 12. Yam KL, Lee D. 1995 Design of modified
611 atmosphere packaging for fresh produce. In *Active*
612 *food packaging*, pp. 55–73. New York, NY: Springer.
- 613 13. Nolen-Hoeksema R. 2014 Defining and determining
614 permeability. *Oilfield Rev.* **26**.
- 615 14. Al-Doury M. 2010 A discussion about hydraulic
616 permeability and permeability. *Pet. Sci. Technol.* **28**,
617 1740–1749. (doi:10.1080/10916460903261715)
- 618 15. Erickson DR. 2015 *Practical handbook of soybean*
619 *processing and utilization*. Elsevier.
- 620 16. Council NR *et al.* 1992 Applications of biotechnology
621 to fermented foods: report of an Ad Hoc panel of
622 the board on science and technology for
623 international development.
- 624 17. De Roos J, Van Der Veken D, De Vuyst L. 2019 The
625 interior surfaces of wooden barrels are an additional
626 microbial inoculation source for lambic beer
627 production. *Appl. Environ. Microbiol.* **85**,
628 e02226–18. (doi:10.1128/AEM.02226-18)
- 629 18. Bear J. 1988 *Dynamics of fluids in porous media*.
630 Courier Corporation.
- 631 19. Woessner WW, Poeter EP. 2020 Hydrogeologic
632 properties of earth materials and principles of
633 groundwater flow (eds J Cherry, P Eileen).
- 634 20. Seo GH, Chung SK, An DS, Lee DS. 2005
635 Permeabilities of Korean earthenware containers
636 and their potential for packaging fresh produce.
637 *Food Sci. Biotechnol.* **14**, 82–88.
- 638 21. Hägg M. 2015 Gas permeation: permeability,
639 permeance, and separation factor. In *Encyclopedia*
640 *of membranes* (eds. E Drioli, L Giorno). pp. 1–4.
- 641 22. Zhang C, Wang Z, Cai Y, Yi C, Yang D, Yuan S. 2013
642 Investigation of gas permeation behavior in facilitated
643 transport membranes: relationship between gas
644 permeance and partial pressure. *Chem. Eng. J.* **225**,
645 744–751. (doi:10.1016/j.cej.2013.03.100)
- 646 23. Civan F. 2010 Effective correlation of apparent
647 gas permeability in tight porous media. *Transp.*
648 *Porous Media* **82**, 375–384. (doi:10.1007/s11242-009-
649 9432-z)
- 650 24. Kim S, No H, Kim U, Cho WS. 2014 A study on
651 sources of pore formation in onggi via the
652 comparison with porcelains. *J. Korean Ceram. Soc.*
653 **51**, 11–18. (doi:10.4191/kcers.2014.51.1.011)
- 654 25. Freeze R, Cherry J. 1979 *Groundwater*. Englewood
655 Cliffs, NJ: Prentice-Hall.
- 656 26. Hornberger GM, Wiberg PL, Raffensperger JP,
657 D'Odorico P. 2014 *Elements of physical hydrology*.
658 JHU Press.
- 659 27. Carman PC. 1937 Fluid flow through granular beds.
660 *Trans. Inst. Chem. Eng.* **15**, 150–166.
- 661 28. Happel J, Brenner H. 2012 *Low Reynolds number*
662 *hydrodynamics: with special applications to*
663 *particulate media*, vol. 1. Springer Science &
664 Business Media.
- 665 29. Ergun S. 1952 Fluid flow through packed columns.
666 *Chem. Eng. Prog.* **48**, 89–94.
- 667 30. Lee DS, Kwon HR, Ha JU. 1997 Estimation of
668 pressure and volume changes for packages of
669 kimchi, a Korean fermented vegetable. *Packaging*
670 *Technol. Sci.: An Int. J.* **10**, 15–32. (doi:10.1002/
671 (SICI)1099-1522(199701/02)10:1<15::AID-PTS378>
672 3.0.CO;2-A)
- 673 31. Che-Othman MH, Millar AH, Taylor NL. 2017
674 Connecting salt stress signalling pathways with
675 salinity-induced changes in mitochondrial metabolic
676 processes in C 3 plants. *Plant Cell Environ.* **40**,
677 2875–2905.
- 678 32. Jacoby RP, Taylor NL, Millar AH. 2011 The role of
679 mitochondrial respiration in salinity tolerance.
680 *Trends Plant Sci.* **16**, 614–623. (doi:10.1016/j.
681 tplants.2011.08.002)
- 682 33. McGovern PE *et al.* 2004 Fermented beverages of
683 pre-and proto-historic China. *Proc. Natl Acad. Sci.*
684 *USA* **101**, 17 593–17 598. (doi:10.1073/pnas.
685 0407921102)
- 686 34. Liu L, Wang J, Levin MJ, Sinnott-Armstrong N,
687 Zhao H, Zhao Y, Shao J, Di N, Zhang TE. 2019
688 The origins of specialized pottery and
689 diverse alcohol fermentation techniques in
690 Early Neolithic China. *Proc. Natl Acad. Sci. USA*
691 **116**, 12 767–12 774. (doi:10.1073/pnas.
692 1902668116)
- 693 35. Ko H, Hu DL. 2020 The physics of tossing fried rice.
694 *J. R. Soc. Interface* **17**, 20190622. (doi:10.1098/rsif.
695 2019.0622)
- 696 36. Kaufman CK. 2006 *Cooking in ancient civilizations*.
697 Greenwood Publishing Group.
- 698 37. Díaz C, Molina AM, Nöhling J, Fischer R. 2013
699 Characterization and dynamic behavior of wild yeast
700 during spontaneous wine fermentation in steel
701 tanks and amphorae. *BioMed Res. Int.* **2013**,
702 540465.
- 703 38. Maga JA. 1989 The contribution of wood to the
704 flavor of alcoholic beverages. *Food Rev. Int.* **5**,
705 39–99. (doi:10.1080/87559128909540844)
- 706 39. Kim S, Hu DL. 2023 Onggi's permeability to carbon
707 dioxide accelerates Kimchi fermentation. Figshare.
708 Available from: https://figshare.com/articles/media/Onggi_s_Permeability_to_Carbon_Dioxide_Accelerates_Kimchi_Fermentation/22230085.